Article

Oxidation of Guanosine Derivatives by a Platinum(IV) Complex: Internal Electron Transfer through Cyclization

Sunhee Choi, Richard B. Cooley, Adelina Voutchkova, Chin Hin Leung, Livia Vastag, and Darcy E. Knowles

J. Am. Chem. Soc., **2005**, 127 (6), 1773-1781• DOI: 10.1021/ja045194n • Publication Date (Web): 20 January 2005

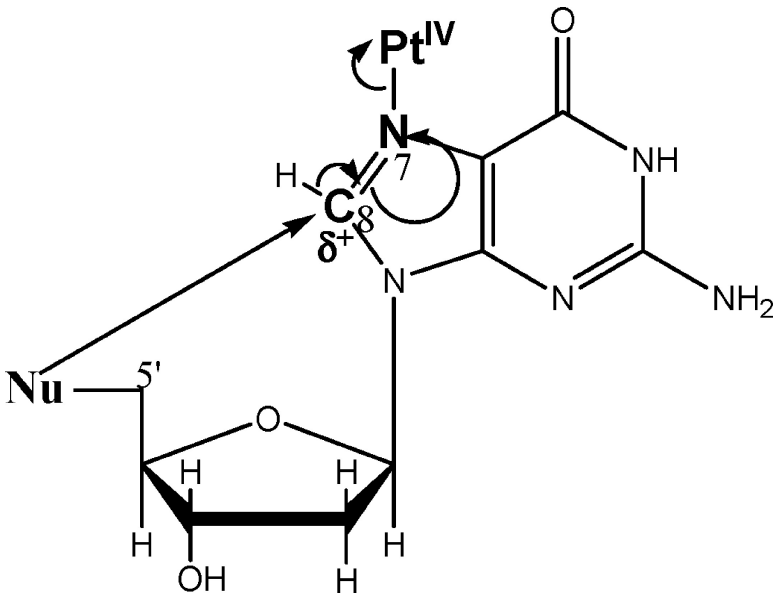

More About This Article

Additional resources and features associated with this article are available within the HTML version:

- Supporting Information
- Links to the 3 articles that cite this article, as of the time of this article download
- Access to high resolution figures
- Links to articles and content related to this article
- Copyright permission to reproduce figures and/or text from this article

View the Full Text HTML

J|A|C|S
ARTICLES
Published on Web 01/20/2005

Oxidation of Guanosine Derivatives by a Platinum(IV) Complex: Internal Electron Transfer through Cyclization

Sunhee Choi,* Richard B. Cooley, Adelina Voutchkova, Chin Hin Leung, Livia Vastag, and Darcy E. Knowles

Contribution from the Department of Chemistry and Biochemistry, Middlebury College, Middlebury, Vermont 05753

Received August 9, 2004; E-mail: choi@middlebury.edu

Abstract: Many transition-metal complexes mediate DNA oxidation in the presence of oxidizing radiation, photosensitizers, or oxidants. The DNA oxidation products depend on the nature of the metal complex and the structure of the DNA. Earlier we reported *trans-d,l*-1,2-diaminocyclohexanetetrachloroplatinum (*trans*-Pt(*d,l*)(1,2-$(NH_2)_2C_6H_{10}$)Cl_4, [$Pt^{IV}Cl_4$(dach)]; dach = diaminocyclohexane) oxidizes 2′-deoxyguanosine 5′-monophosphate (5′-dGMP) to 7,8-dihydro-8-oxo-2′-deoxyguanosine 5′-monophosphate (8-oxo-5′-dGMP) stoichiometrically. In this paper we report that [$Pt^{IV}Cl_4$(dach)] also oxidizes 2′-deoxyguanosine 3′-monophosphate (3′-dGMP) stoichiometrically. The final oxidation product is not 8-oxo-3′-dGMP, but cyclic (5′-O-C8)-3′-dGMP. The reaction was studied by high-performance liquid chromatography, ^1H and ^{31}P nuclear magnetic resonance, and matrix-assisted laser desorption ionization time-of-flight mass spectrometry. The proposed mechanism involves Pt^{IV} binding to N7 of 3′-dGMP followed by nucleophilic attack of a 5′-hydroxyl oxygen to C8 of G and an inner-sphere, $2e^-$ transfer to produce cyclic (5′-O-C8)-3′-dGMP and [$Pt^{II}Cl_2$(dach)]. The same mechanism applies to 5′-d[GTTTT]-3′, where the 5′-dG is oxidized to cyclic (5′-O-C8)-dG. The Pt^{IV} complex binds to N7 of guanine in cGMP, 9-Mxan, 5′-d[TTGTT]-3′, and 5′-d[TTTTG]-3′, but no subsequent transfer of electrons occurs in these. The results indicate that a good nucleophilic group at the 5′ position is required for the redox reaction between guanosine and the Pt^{IV} complex.

Introduction

Many transition-metal complexes mediate DNA oxidation in the presence of oxidizing radiation, photosensitizers, or oxidants.[1] Among the four DNA bases, guanine (G) is the most easily oxidizable base because it has the lowest redox (1.29 V vs NHE) and ionization (7.75 eV) potentials.[2] The major oxidation products of G widely depend on the oxidation mechanism and the structures of DNA.[3] In the presence of oxidants (O_2, H_2O_2, or SO_3^{2-}), complexes of Cr^{IV}, Mn^{II}, Fe^{III}, Co^{II}, Ni^{II}, and Cu^{II} abstract $1e^-$ from G and generate the G radical cation, $G^{\bullet+}$. $G^{\bullet+}$ undergoes a series of reactions to produce 2-amino-5-[(2-deoxy-β-D-*erythro*-pentofuranosyl)amino]-4*H*-imidazol-4-one (imidazolone, Iz) or 2,2-diamino-4-[2-deoxy-β-D-*erythro*-pentofuranosyl)amino]-2,5-dihydrooxazol-5-one (oxazolone, Oxz) when G is in mononucleotides and single-stranded DNA. However, in double-stranded DNA, $G^{\bullet+}$ becomes 8-oxo-G. The oxomanganese porphyrin activated by $KHSO_5$ generates Mn^V=O, which abstracts $2e^-$ from G to generate the G cation, G^+.[4] G^+ becomes Iz and dehydroguanidinohydantoin when G is from 2′-deoxyguanosine monophosphate (dGMP) and oligonucleotides, respectively.

We recently reported that a Pt^{IV} complex, *trans-d,l*-1,2-diaminocyclohexanetetrachloroplatinum (*trans*-Pt(*d,l*)(1,2-$(NH_2)_2C_6H_{10}$)Cl_4, [$Pt^{IV}Cl_4$(dach)]; dach = diaminocyclohexane), oxidizes 5′-dGMP to 7,8-dihydro-8-oxo-2′-deoxyguanosine 5′-monophosphate (8-oxo-5′-dGMP).[5a,b] The mechanism involves Pt^{IV} binding to N7 of 5′-dGMP followed by cyclization of a phosphate oxygen to C8 of 5′-dGMP, accompanied by an inner-sphere, $2e^-$ transfer to produce a cyclic phosphodiester intermediate, 8-hydroxyguanosine, cyclic 5′,8-(hydrogen phosphate). This intermediate slowly converts to 8-oxo-5′-dGMP by reacting with solvent H_2O. The overall reaction generates two protons, one 8-oxo-5′-dGMP, and two chlorides when one Pt^{IV} and one 5′-dGMP are allowed to react.

To our knowledge, this is the only system in which 8-oxo-G is generated cleanly and stoichiometrically from the transition-metal oxidation of a mononucleotide. Although it is reported that Ru^{IV}=O complexes oxidize guanine via an inner-sphere, oxygen atom transfer to produce 8-oxo-G,[6] the detailed mechanism and stoichiometry have not been reported. The autoxi-

(1) (a) Sies, H. *Oxidative Stress: Oxidants and Antioxidants*; Academic Press: London, 1991. (b) Marnett, L. J., Burcham, P. C. *Chem. Res. Toxicol.* **1993**, *6*, 771−785. (c) Cadet, J. In *DNA Adducts: Identification and Biological Significance*; Hemminki, K., Dipple, A., Shuker, D. G. E., Kadlubar, F. F., Segerbäck, D., Bartsch, H., Eds.; IARC Scientific Publication No. 125; IARC: Lyon, 1994; pp 245−276.

(2) (a) Steenken, S., Jovanovic, S. *J. Am. Chem. Soc.* **1997**, *119*, 617−618. (b) Candeias, L. P.; Steenken, S. *J. Am. Chem. Soc.* **1989**, *111*, 1094−1099.

(3) (a) Burrows, C. J.; Muller, J. G. *Chem. Rev.* **1998**, *98*, 1109−1151. (b) Pyle, A. M.; Barton, J. K. *Prog. Inorg. Chem.: Bioinorg. Chem.* **1990**, *38*, 413−475. (c) Chow, C. S.; Barton, J. K. *Methods Enzymol.* **1992**, *212*, 219−242.

(4) (a) Vialas, C.; Pratviel, G.; Claparols C.; Meunier, B. *J. Am. Chem. Soc.* **1998**, *120*, 11548−11553. (b) Vialas, C.; Claparols C.; Pratviel, G.; Meunier, B. *J. Am. Chem. Soc.* **2000**, *122*, 2157−2167. (c) Meunier, B. *J. Inorg. Biochem.* **2001**, *86*, 74.

(5) (a) Choi, S.; Cooley, R. B.; Hakemian, A. S.; Larrabee, Y. C.; Bunt, R. C.; Maupaus, S. D.; Muller, J. G.; Burrows, C. J. *J. Am. Chem. Soc.* **2004**, *126*, 591−598. (b) Choi, S.; Orbai, L.; Padgett, E. J.; Delaney, S.; Hakemian, A. S. *Inorg. Chem.* **2001**, *40*, 5481−5482. (c) Choi, S.; Mahalingaiah, S.; Delaney, S.; Neale, N. R.; Masood, S. *Inorg. Chem.* **1999**, *38*, 1800−1805.

10.1021/ja045194n CCC: $30.25

Chart 1. Structures of the Guanine Derivatives Studied

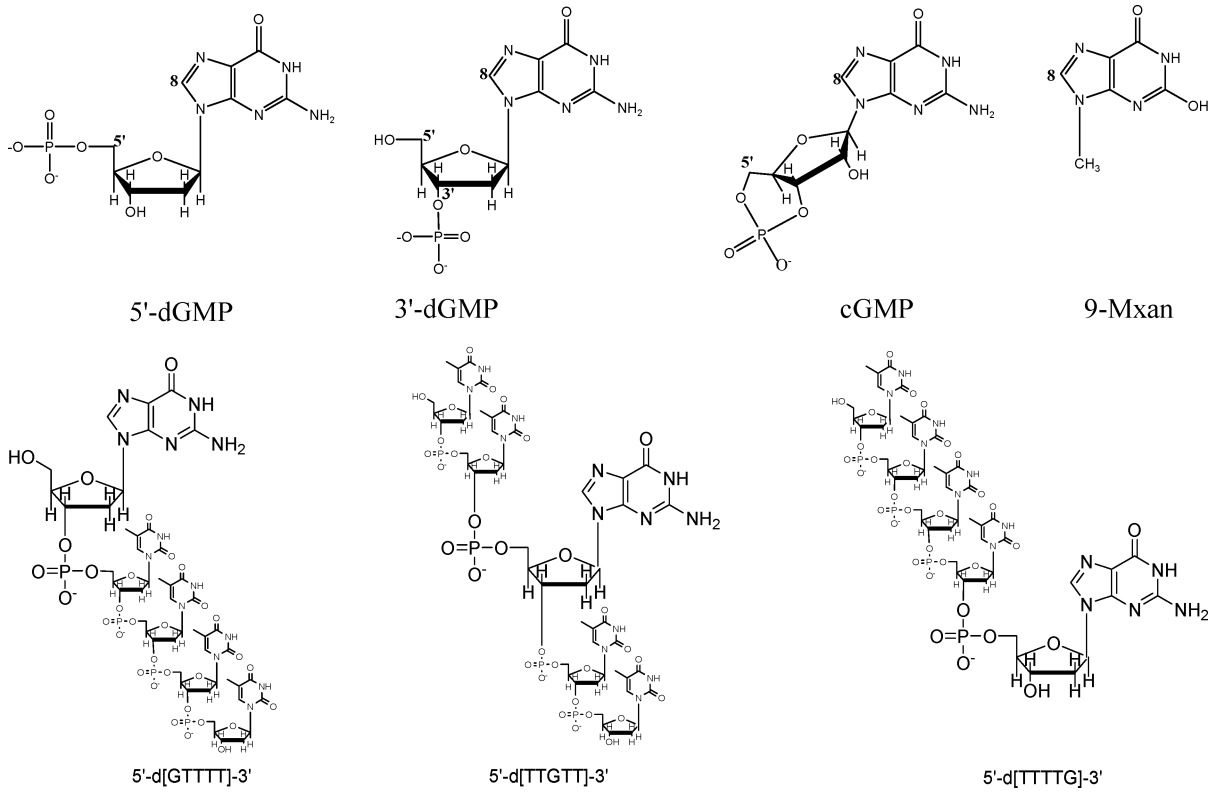

dation of a series of 6-oxopurines by $[Ru^{III}(NH_3)_5]$ to 8-ketonucleosides involves two sequential $1e^-$, $1H^+$ oxidations.[7] The Ru^{III} complex binds to N7 of inosine, leading to deprotonation of H8 and transfer of $1e^-$ to Ru^{III}, and generates a radical at C8. This radical is attacked by water, and undergoes a second $1e^-$, $1H^+$ oxidation to produce an 8-ketonucleoside.

The stoichiometric oxidation of a guanosine monomer to 8-oxo-G by $[Pt^{IV}Cl_4(dach)]$ is new chemistry, and therefore, many questions remain to be answered. Our immediate question was, how will $[Pt^{IV}Cl_4(dach)]$ react with other monomeric guanosine derivatives such as 3′-dGMP, cGMP, and 9-Mxan? What about oligonucleotides? A detailed mechanism of the redox reaction between $[Pt^{IV}Cl_4(dach)]$ and 3′-dGMP is proposed on the basis of UV/vis, HPLC, ^1H and ^{31}P NMR, and MS studies. The mechanism involves Pt^{IV} binding to N7 of dG followed by cyclization of a hydroxyl oxygen at the 5′-position to C8 of dG. The same mechanism applies to 5′-d[GTTTT]-3′, where 5′-dG is oxidized to cyclic (5′-O-C8)-dG. Although the Pt^{IV} complex binds to N7 of guanine in cGMP, 9-Mxan, 5′-d[TTGTT]-3′, and 5′-d[TTTTG]-3′, no subsequent transfer of electrons occurs in these, however. The results indicate that a good nucleophilic group at the 5′ position is required for the redox reaction between guanosine and the Pt^{IV} complex.

See Chart 1 for the structures of the guanine derivatives studied.

Results

3′-dGMP. FTIR, UV/vis, and ^1H NMR spectra showed that $[Pt^{IV}Cl_4(dach)]$ reacts with 3′-dGMP essentially the same way as with 5′-dGMP except for its kinetic rate and the final oxidation product. Figure 1 displays the absorbance at 360 nm due to $[Pt^{IV}Cl_4(dach)]$ over time. The different rates in the decrease of absorbance reveal that Pt^{IV} is reduced faster by 3′-dGMP than by 5′-dGMP. The detailed kinetic data, however, will be discussed in a separate paper. The final reaction mixture of $[Pt^{IV}Cl_4(dach)]$/3′-dGMP contained orange crystals identified as $[Pt^{II}Cl_2(dach)]$ by FTIR,[5] indicating that a $2e^-$ redox reaction occurred between $[Pt^{IV}Cl_4(dach)]$ and 3′-dGMP similar to that of the $[Pt^{IV}Cl_4(dach)]$/5′-dGMP reaction. However, ^1H and ^{31}P NMR, HPLC, and MS showed that the oxidized species of 3′-dGMP is not 8-oxo-3′-dGMP (vide infra).

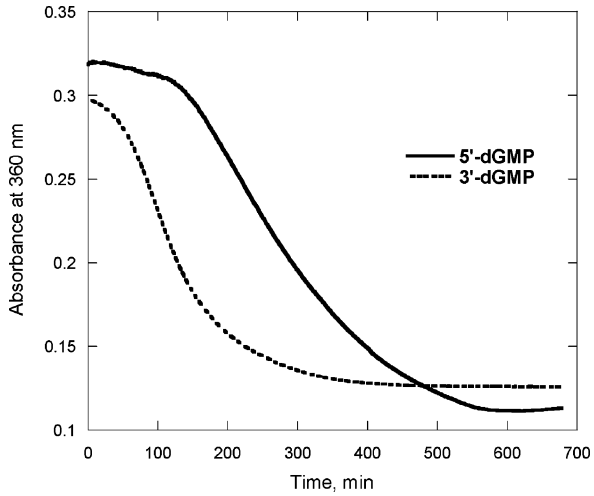

Figure 1. A_{360} vs time for the reaction of 10 mM $[Pt^{IV}Cl_4(dach)]$ with 20 mM 5′-dGMP and 3′-dGMP at pH 8.6 ($t = 0$) and 37 °C.

(6) (a) Farrer, B. T.; Thorp, H. H. *Inorg. Chem.* **2000**, *39*, 44−49. (b) Carter, P. J.; Cheng, C.-C.; Thorp, H. H. *J. Am. Chem. Soc.* **1998**, *120*, 632−642. (c) Carter, C. P.; Cheng, C.-C.; Thorp, H. H. *Inorg. Chem.* **1996**, *35*, 3348−3354. (d) Cheng, C.-C., Goll, J. G.; Neyhart, G. A.; Welch, T. W.; Singh, P.; Thorp, H. H. *J. Am. Chem. Soc.* **1995**, *117*, 2970−2980.
(7) (a) Clarke, M. J.; Morrissey, P. E. *Inorg. Chim. Acta* **1984**, *80*, L69−70. (b) Gariepy, K. C.; Curtin, M. A.; Clarke, M. J. *J. Am. Chem. Soc.* **1989**, *111*, 4947−4952.

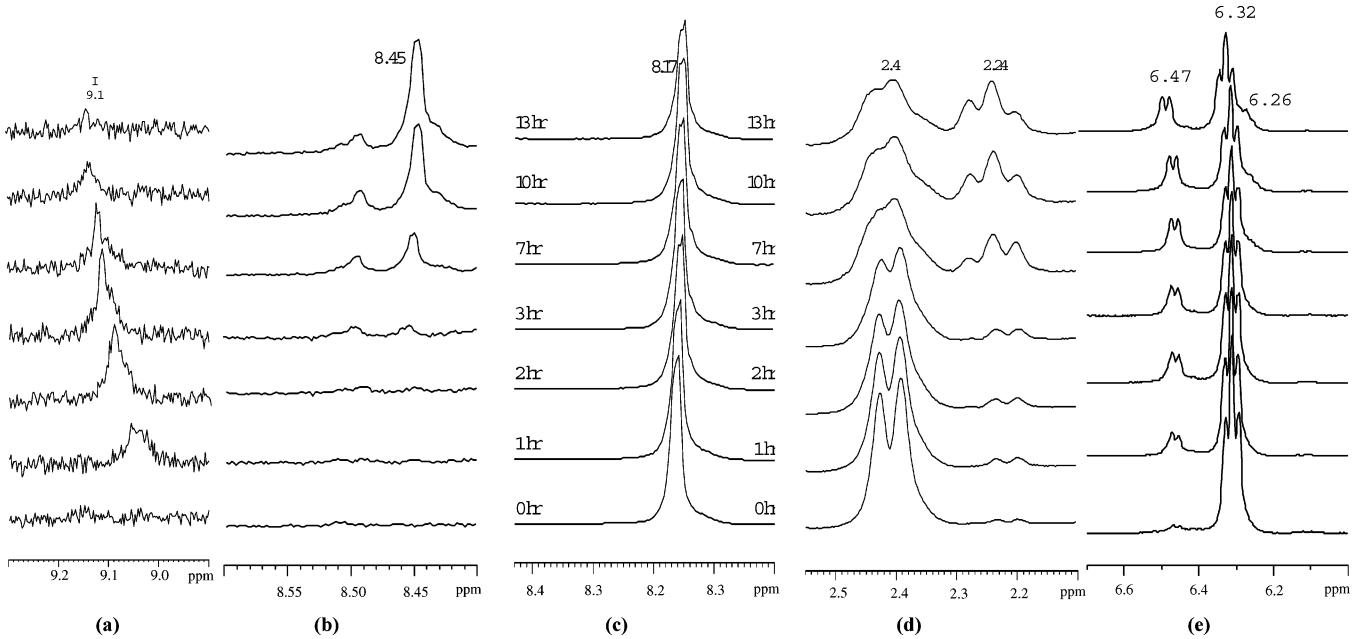

Figure 2. ^{1}H NMR spectra of the reaction of 10 mM [$Pt^{IV}Cl_4$(dach)] with 20 mM 3′-dGMP at pH 8.6 ($t = 0$) and 37 °C. The gradual downfield shift of the 9 ppm peak as the reaction progresses is due to the lowering of the pH as the reaction proceeds.

The time course of the reaction of [$Pt^{IV}Cl_4$(dach)]/3′-dGMP was monitored by ^{1}H NMR spectroscopy. The multiplet peak at 9.11 ppm (Figure 2a) due to the H8 of Pt^{IV} bound to the N7 of guanine[5a,8] appears after 1 h, grows in intensity, and disappears after 14 h. This indicates that the Pt^{IV}−G adduct is an intermediate. After 3 h of reaction, a new peak at 8.45 ppm (Figure 2b) appears whose peak intensity continuously grows with a concomitant decrease in the intensity of the 8.17 ppm peak (Figure 2c) due to H8 of free-3′-dGMP. The 8.45 ppm peak is assigned to H8 of the Pt^{II}−3′-dGMP adduct.[5a,8] This adduct was produced from the reaction of hydrolyzed [$Pt^{II}Cl_2$-(dach)] with free 3′-dGMP. The [$Pt^{II}Cl_2$(dach)] complex appears after 1 h at 2.24 ppm[5a] (Figure 2d), hydrolyzes, and binds to 3′-dGMP. The 2.4 ppm peak is due to [$Pt^{IV}Cl_4$(dach)], whose intensity decreases over time. Another growing peak at 8.49 ppm is tentatively assigned to the Pt^{II}−(5′-O-C8)-3′-dGMP adduct (vide infra).

The peak at 6.32 ppm (Figure 2e) is due to the H1′ of free 3′-dGMP, and its peak intensity decreases as the reaction progresses. The new peak at 6.26 ppm is assigned to the Pt^{II}−dGMP adduct.[5a] The other new peak centered at 6.47 ppm appears at the same time as the [$Pt^{II}Cl_2$(dach)] peak at 2.24 ppm. Its peak intensity grows and reaches a maximum, indicating that this peak is due to the final product of oxidized 3′-dGMP (denoted as **II**). There is no indication of 8-oxo-3′-dGMP, whose H1′ should appear 0.1 ppm upfield of the H1′ of free 3′-dGMP. The H1′ peaks of free 5′-dGMP and 8-oxo-5′-dGMP appear at 6.46 and 6.36 ppm, respectively.[5a]

The time course of ^{31}P NMR spectra of the reaction mixture indicates the phosphorus atom in **II** is in an environment similar

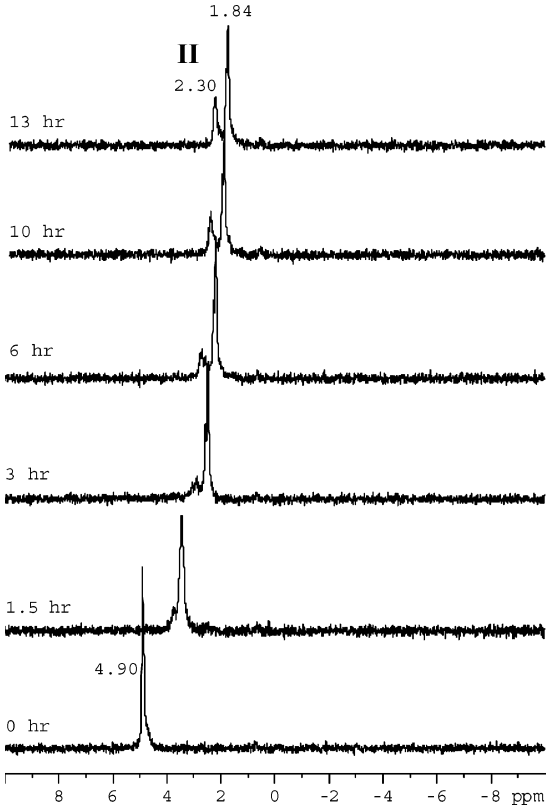

Figure 3. ^{31}P NMR spectra of 10 mM [$Pt^{IV}Cl_4$(dach)] with 20 mM 3′-dGMP at pH 8.6 ($t = 0$) and 37 °C.

to that of the phosphorus atom in 3′-dGMP (Figure 3). After 1.5 h, the new peak observed at 0.46 ppm downfield from the main peak (4.9 ppm at 0 h) is due to **II**, and its intensity grows with time. Because the pH drops from 8.6 ($t = 0$ h) to 4 ($t =$ 14 h), both peaks gradually shift upfield as the reaction progresses. It is known that both inorganic and nucleotide phosphates shift upfield at lower pH.[9] This also indicates that the phosphate group in **II** is not a phosphodiester whose ^{31}P NMR peak at −5.5 ppm is not sensitive to pH.[5a]

(8) (a) Roat, R. M.; Reedijk, J. *J. Inorg. Biochem.* **1993**, *52*, 263−274. (b) Talman, E. G.; Brüning, W.; Reedijk, J.; Spek, A. L.; Veldman, N. *Inorg. Chem.* **1997**, *36*, 854−861. (c) van der Veer, J. L.; Peters, A. R.; Reedijk, J. *J. Inorg. Biochem.* **1986**, *26*, 137−142. (d) Roat, R. M.; Jerardi, M. J.; Kopay, C. B.; Heath, D. C.; Clark, J. A.; DeMars, J. A.; Weaver, J. M.; Bezemer, E.; Reedijk, J. *J. Chem. Soc., Dalton Trans.* **1997**, 3615−3621. (e) Galanski, M.; Keppler, B. K. *Inorg. Chim. Acta* **2000**, *300*−*302*, 783−789. (f) Ali, M. S.; Khokhar, A. R. *J. Inorg. Biochem.* **2003**, *96*, 452−456.

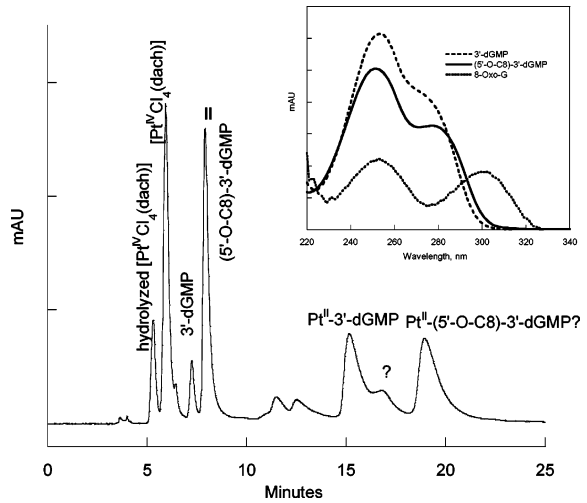

Figure 4. HPLC chromatogram (DAD, $\lambda = 260$ nm) of the 10 h reaction of 20 mM $[Pt^{IV}Cl_4(dach)]$ with 20 mM 3′-dGMP at pH 8.6 ($t = 0$) and 37 °C.

The HPLC results (Figure 4) confirm that there is no 8-oxo-3′-dGMP in the final reaction mixture. Neither HPLC/DAD (photodiode array detector) nor HPLC/ECD (electro chemical detector) shows a peak due to 8-oxo-G. A new peak with a retention time of 7.9 min grows in its intensity and reaches a maximum around 5 h, which is the same trend as the peak at 6.47 ppm in the ^{1}H NMR spectrum (Figure 2e). Therefore, we assign this peak to product **II**. The UV spectrum of this peak obtained directly from HPLC/DAD has λ_{max} at 251 and 277 nm, different from those of free 3′-dGMP ($\lambda_{max} = 253$ nm, shoulder at 265 nm) and 8-oxo-dGMP ($\lambda_{max} = 252$ and 280 nm). The UV spectrum is similar to that of cyclic (5′-O-C8)-G,[10] suggesting that **II** may be cyclic (5′-O-C8)-3′-dGMP. The peak at 15 min is assigned to the Pt^{II}−3′-dGMP adduct by comparing the retention time of the authentic Pt^{II}−3′-dGMP. The peak at 19 min is tentatively assigned to the Pt^{II}−(5′-O-C8)-3′-dGMP adduct.

The 7.9 min peak (**II**) in Figure 4 was collected by HPLC and analyzed by ^{1}H NMR and MS. ^{1}H NMR (Figure 5) shows one distinct doublet at 6.48 ppm, and only minor peaks at 6.31 ppm (triplet) and 7.98 ppm (singlet) from 3′-dGMP impurities. This indicates that the new HPLC peak at 7.9 min is the same product observed at 6.47 ppm in the ^{1}H NMR spectrum shown in Figure 2b. This also shows that the oxidized product has no H8 proton, which is the case for cyclic (5′-O-C8)-dGMP. The doublet of the 6.48 ppm peak is consistent with the cyclic nature of **II**. According to the Karplus correlation, the coupling constant between neighboring protons is 0 when their dihedral angle is near 85°.[11] The formation of the cycle prohibits rotation of the H2′−H1′ dihedral angle, and thus, the angle is "frozen" in a state such that the H1′ proton only couples with one of the H2′ protons, not both. Free 3′-dGMP, however, is capable of rotating this dihedral angle during the process of switching from the 3′-*endo*, 2′-*exo* sugar conformation to the 3′-*exo*, 2′-*endo* conformation, allowing the H1′ proton to couple with both the H2′ and H2″ protons, giving a triplet peak.

Mass spectrometry was done to further characterize **II** and compared to that of 3′-dGMP using MALDI-TOF-MS. Figure 6b displays $m/z = 345.2501$ for **II**, the same m/z as that of (5′-O-C8)-3′-dGMP and two units less than that of 3′-dGMP ($m/z = 347.1861$, Figure 6a) as expected due to the loss of two H atoms during the oxidation process.

The concentration of 3′-dGMP at various time intervals was obtained by comparison of calibration curves of authentic 3′-dGMP with HPLC chromatograms obtained with DAD monitoring at 260 nm. The concentration of $[Pt^{IV}Cl_4(dach)]$ was obtained from the relative intensity of the 2.42 ppm peak due to $[Pt^{IV}Cl_4(dach)]$ compared to the internal standard, 3-(trimethylsilyl)propionic acid (TSP), peak at 0 ppm. The concentration of (5′-O-C8)-3′-dGMP was obtained from the calibration curve of the ^{1}H NMR integration of the 6.47 ppm peak relative to the H1′ peak of authentic 3′-dGMP using TSP as an internal standard. The concentrations of 3′-dGMP and $[Pt^{IV}Cl_4(dach)]$ reacted, along with cyclic (5′-O-C8)-3′-dGMP produced, are displayed in Figure 7. The concentrations of reacted 3′-dGMP and $[Pt^{IV}Cl_4(dach)]$ are the same within experimental error, indicating that 1 equiv of 3′-dGMP reacts with 1 equiv of $[Pt^{IV}Cl_4(dach)]$. The concentration−time profile of cyclic (5′-O-C8)-3′-dGMP is symmetrical to those of the reactants, indicating that 1 equiv of $[Pt^{IV}Cl_4(dach)]$ converts 1 equiv of 3′-dGMP to 1 equiv of cyclic (5′-O-C8)-3′-dGMP. For the 10 h reaction mixture of 10 mM $[Pt^{IV}Cl_4(dach)]$ and 20 mM dGMP (pH 8.6 at $t = 0$), approximately 6 mM $[Pt^{IV}Cl_4(dach)]$ and 3′-dGMP were consumed to produce 6 mM (5′-O-C8)-3′-dGMP. The same results were obtained from the ^{31}P NMR data (Figure 3). The integration ratio of the 2.3 ppm peak due to cyclic (5′-O-C8)-3′-dGMP and 1.84 ppm peak due to free 3′-dGMP is 1:2.3, indicating that 30% of the 20 mM 3′-dGMP (6 mM) was converted to cyclic (5′-O-C8)-3′-dGMP. Therefore, the overall reaction can be written as follows:

$$[Pt^{IV}Cl_4(dach)] + 3'\text{-dGMP} \rightarrow [Pt^{II}Cl_2(dach)] + \text{cyclic (5′-O-C8)-3′-dGMP} + 2H^+ + 2Cl^- \quad (1)$$

Indeed, the pH of the solution dropped from 8.6 to 4.0 in 14 h of reaction, and the chloride concentrations increased stoichiometrically.

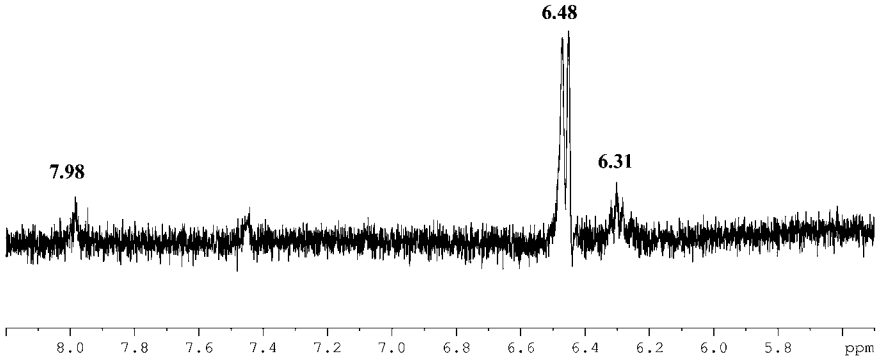

Figure 5. ^{1}H NMR spectrum of **II** (fraction at 7.9 min in Figure 6).

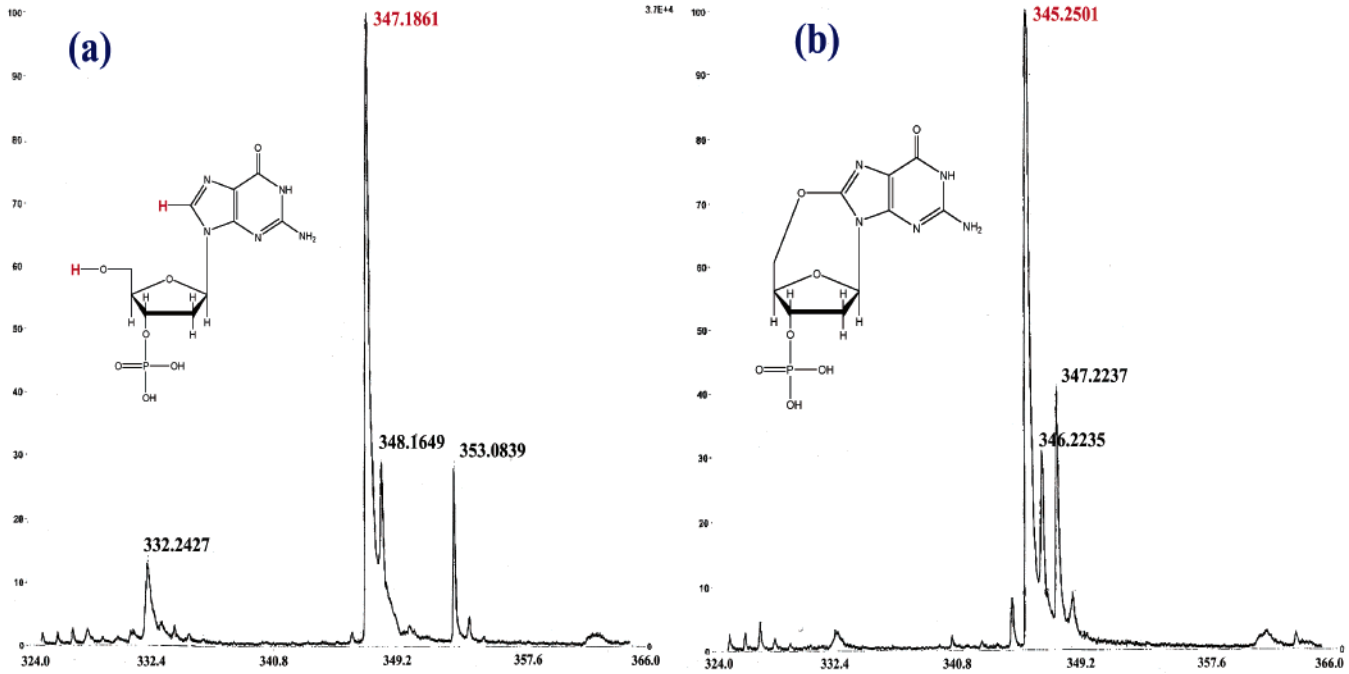

Figure 6. MALDI-TOF-MS spectrum of (a) 3′-dGMP and (b) **II**, (5′-O-C8)-3′-dGMP.

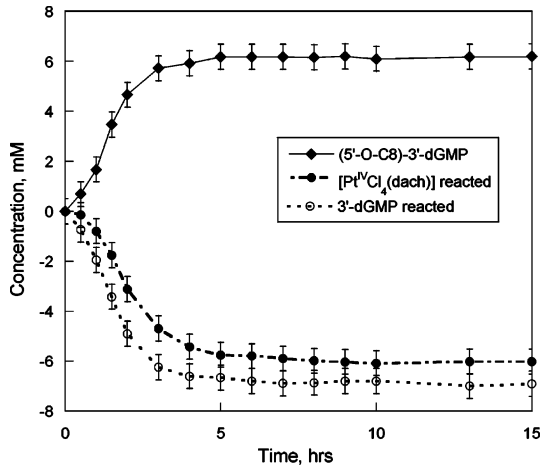

Figure 7. Time-dependent concentrations of $[Pt^{IV}Cl_4(dach)]$ and 3′-dGMP consumed and (5′-O-C8)-3′-dGMP produced from the reaction of 10 mM $[Pt^{IV}Cl_4(dach)]$ with 20 mM 3′-dGMP at pH 8.6 ($t = 0$) and 37 °C.

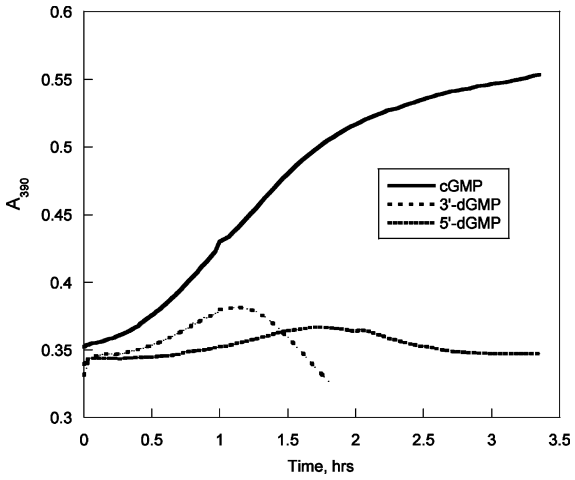

Figure 8. Absorbance at 390 nm vs time for the reaction of 5 mM $[Pt^{IV}Cl_4(dach)]$ with 20 mM cGMP, 3′-dGMP, or 5′-dGMP at pH 7.6 ($t = 0$) and 47 °C.

cGMP and 9-Mxan. The $[Pt^{IV}Cl_4(dach)]$ reaction with cGMP or 9-Mxan did not produce orange crystals of $[Pt^{II}Cl_2(dach)]$, indicating that there was no redox reaction. Figure 8 displays the absorbance at 390 nm due to the $Pt^{IV}-G$ adduct over time. The absorbances of 5′-dGMP and 3′-dGMP increase to maxima and decrease, confirming that the $Pt^{IV}-$dGMP adducts are the intermediates. On the other hand, the absorbance of the cGMP reaction increases to a maximum without decreasing. The intensities of the 9.1 and 8.55 ppm peaks due to H8 of cGMP (Figure 9) and 9-Mxan (Figure 10), respectively, also continuously increase without decreasing. These results indicate that $Pt^{IV}-$cGMP and $Pt^{IV}-$9-Mxan adducts are the final products.

5′-d[GTTTT]-3′, 5′-d[TTTTG]-3′, and 5′-d[TTGTT]-3′. To understand the effect of guanine sites in oligonucleotides, 5′-d[GTTTT]-3′, 5′-d[TTTTG]-3′, and 5′-d[TTGTT]-3′ were studied. Orange crystals were detected from the reaction of $[Pt^{IV}Cl_4(dach)]$ with 5′-d[GTTTT]-3′, but not with 5′-d[TTTTG]-3′ or 5′-d[TTGTT]-3′. The orange crystals were identified as $[Pt^{II}Cl_2(dach)]$ by FTIR. This indicates that a redox reaction occurred between $[Pt^{IV}Cl_4(dach)]$ and 5′-d[GTTTT]-3′, but not with 5′-d[TTTTG]-3′ or 5′-d[TTGTT]-3′.

The ^{1}H NMR spectra of the reactions of all three oligonucleotides with $[Pt^{IV}Cl_4(dach)]$ display a new peak around 9.0−11 ppm corresponding to the H8 of $Pt^{IV}-G$. The intensity of this peak for the 5′-d[GTTTT] reaction reaches a maximum at 24 h and gradually decreases (Figure 11a), indicating that the $Pt^{IV}-G$ adduct is an intermediate. However, it continuously grows for the reaction of 5′-d[TTGTT]-3′ and 5′-d[TTTTG] (Figure 11b), indicating that the $Pt^{IV}-G$ adduct is the final product.

(9) (a) Bose, R. N.; Fonkeng, B. S.; Moghaddas, S.; Stroup, D. *Nucleic Acids Res.* **1998**, *26*, 1588−1596. (b) Robitaille, P.-M. L.; Robitaille, P. A.; Brown, G. G., Jr.; Brown, G. G. *J. Magn. Reson.* **1991**, *92*, 73−84.
(10) Guengerich, F. P.; Mundkowski, R. G.; Voehler, M.; Kadlubar, F. F. *Chem. Res. Toxicol.* **1999**, *12*, 906−916.
(11) Silverstein, R. M.; Bassler, G. C.; Morrill, T. C. *Spectrometric Identification of Organic Compounds*. 5th ed.; John Wiley & Sons: New York, 1999; pp 196−197.

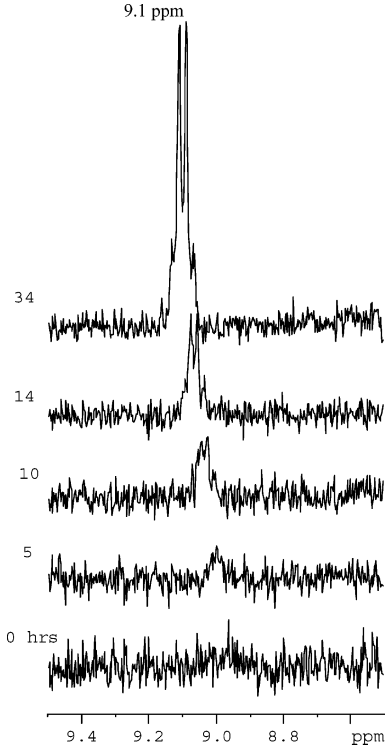

Figure 9. Time-dependent ^{1}H NMR spectra of the reaction of 5 mM [$Pt^{IV}Cl_4$(dach)] with 20 mM cGMP at pH 8.8 (t = 0) and 50 °C.

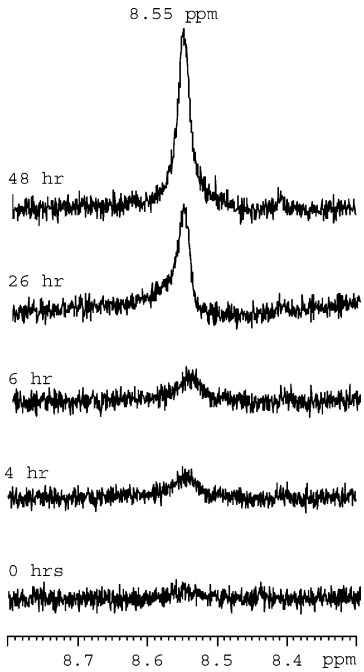

Figure 10. Time-dependent ^{1}H NMR spectra of the reaction of 2 mM [$Pt^{IV}Cl_4$(dach)] with 2 mM 9-Mxan at pH 7.0 (t = 0) and 50 °C.

The ^{31}P NMR spectrum of the 5′-d[Gp*TpTpTpT]-3′ reaction shows a new peak at 1.3 ppm (Figure 12a). This new peak is attributed to the phosphorus (P*) at 3′ of G that shifts as a result of the cyclic (5′-O-C8)-dGp* formation. A similar shift was observed in the study of 3′-dGMP (Figure 3). The integration ratio of the two ^{31}P peaks is 1:3.5, indicating 22% of the total phosphorus belongs to a cyclized nucleotide. Since the cyclization only occurs at G with 22% of the total phosphorus, about 88% (0.22/0.25 = 0.88) of G was converted to cyclic G after 3 days of reaction. The ^{31}P NMR spectra of the 5′-d[TTTTG]-3′ or 5′-d[TTGTT]-3′ reaction did not show any new peak (Figure 12b).

The HPLC chromatogram of the digested [$Pt^{IV}Cl_4$(dach)]/5′-d[GTTTT]-3′ reaction shows a peak at 14.2 min (Figure 13), whose UV spectrum matches that of a cyclic (5′-O-C8)-G (λ_{max} = 251 and 272 nm). There was no sign of an 8-oxo-G peak. The HPLC chromatograms of the digested [$Pt^{IV}Cl_4$(dach)]/5′-d[TTGTT]-3′ or [$Pt^{IV}Cl_4$(dach)]/5′-d[TTTTG]-3′ did not show a cyclic (5′-O-C8)-G or 8-oxo-G peak. The concentrations of reacted G were calculated using a calibration curve. After 2 days of reaction, about 50%, 23%, and 9% of G in 5′-d[GTTTT]-3′, 5′-d[TTTTG]-3′, and 5′-d[TTGTT]-3′, respectively, reacted with [$Pt^{IV}Cl_4$(dach)].

Discussion

The above results led us to propose the redox mechanism for the reaction of [$Pt^{IV}Cl_4$(dach)] with 3′-dGMP or 5′-d[GTTTT]-3′ in Scheme 1. The first step is loss of Cl^- from [$Pt^{IV}Cl_4$(dach)] followed by binding to N7-G. Although we show the axial chloride substituted with dGMP, it is also possible that the equatorial chloride could be replaced. The next step involves nucleophilic attack at C8 by a hydroxyl group and an inner-sphere, $2e^-$ transfer from bound dG to Pt^{IV} to produce the (5′-O-C8)-cyclic ether and [$Pt^{II}Cl_2$(dach)]. [$Pt^{II}Cl_2$(dach)] reacts with free 3′-dGMP and cyclic (5′-O-C8)-3′-dGMP product, and produces Pt^{II}−3′-dGMP and Pt^{II}−(5′-O-C8)-3′-dGMP adducts. Unlike cyclic phosphodiester, the cyclic ether does not hydrolyze. The same oxidation mechanism applies to the guanosine in 5′-d[GTTTT]-3′. The free hydroxyl group at the 5′-position initiates cyclization accompanied by an inner-sphere electron transfer.

The formation of a cyclic ether by nucleophilic attack of the 5′-hydroxyl at a carbon has been observed by other researchers. When guanosine was reacted with 2,4-dinitrophenoxyamine, it produced an N7-NH_2G cation intermediate (positive charge at C8) that became cyclic (5′-O-C8)-G by the 5′-OH attack on C8.[10] Very recently it has been reported that [$PtCl_2(H_2C{=}CH_2)]_2$ catalyzes the synthesis of cyclic ethers (five- or six-membered) via the intramolecular addition of the O−H bond of an alcohol across the C=C bond of a pendant olefin.[12] The Pt^{II} complex binds to the C=C bond, initiating the attack of the OH group to one of the carbons of C=C. The principle of our mechanism seems basically the same as in these cases. The hydroxyl group attacks the positively charged or polarized carbon to form a cyclic ether.

For cGMP, 9-Mxan, 5′-d[TTGTT]-3′, or 5′-d[TTTTG]-3′ the cyclization−electron-transfer mechanism does not apply. The mononucleotides do not have a free nucleophilic group at the 5′ position for cyclization. Although the oligonucleotides contain a 5′-phosphodiester, steric hindrance or base stacking interactions prevent the phosphodiester from adopting the proper conformation to attack G. Therefore, Pt^{IV} simply binds to N7-G without a further redox reaction. In earlier work[5b] we reported that the G in a double-stranded oligonucleotide, 5′-d[TGATCG-GTGCGTCTGAGACT]-3′, was oxidized to 8-oxo-G by [$Pt^{IV}Cl_4$(dach)]. However, this result was erroneous because it was obtained without gel filtration prior to enzyme digestion. When the reaction was digested without gel filtration, a small amount

(12) Qian, H.; Han, X.; Widenhoefer, R. A. *J. Am. Chem. Soc.* **2004**, *126*, 9536−9537.

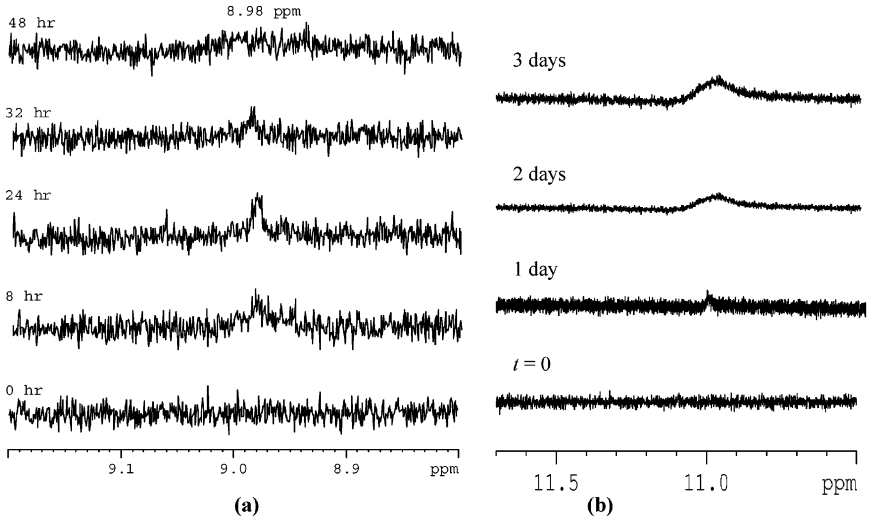

Figure 11. ^{1}H spectra of the reaction of 0.3 mM $[Pt^{IV}Cl_4(dach)]$ with 0.3 mM (a) 5′-d[GTTTT]-3′ and (b) 5′-d[TTGTT]-3′ or 5′-d[TTTTG]-3′ at pH 7.4 and 37 °C.

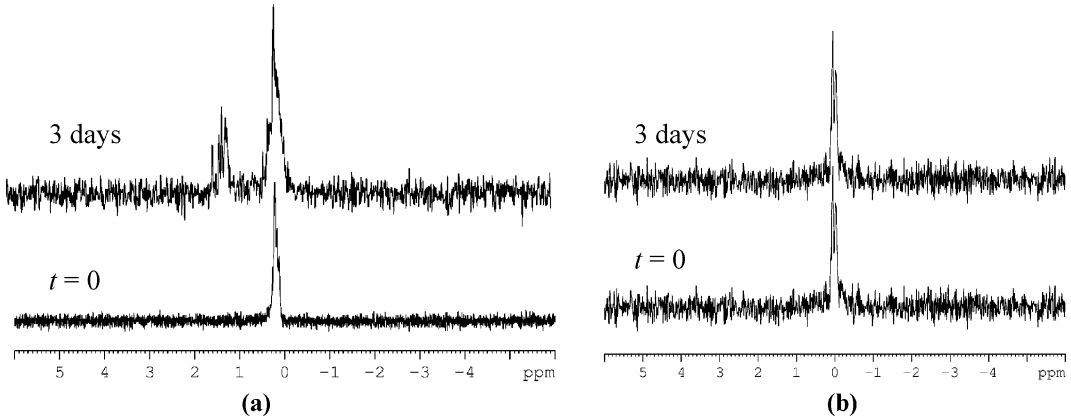

Figure 12. ^{31}P NMR spectra of the reaction of 0.3 mM $[Pt^{IV}Cl_4(dach)]$ with 0.3 mM (a) 5′-d[GTTTT]-3′ and (b) 5′-d[TTGTT]-3′ or 5′-d[TTTTG]-3′ at pH 7.4 ($t = 0$) and 37 °C.

Scheme 1. Proposed Mechanism for the Reaction of $[Pt^{IV}Cl_4(dach)]$ with 3′-dGMP or 5′-d[GTTTT]-3′

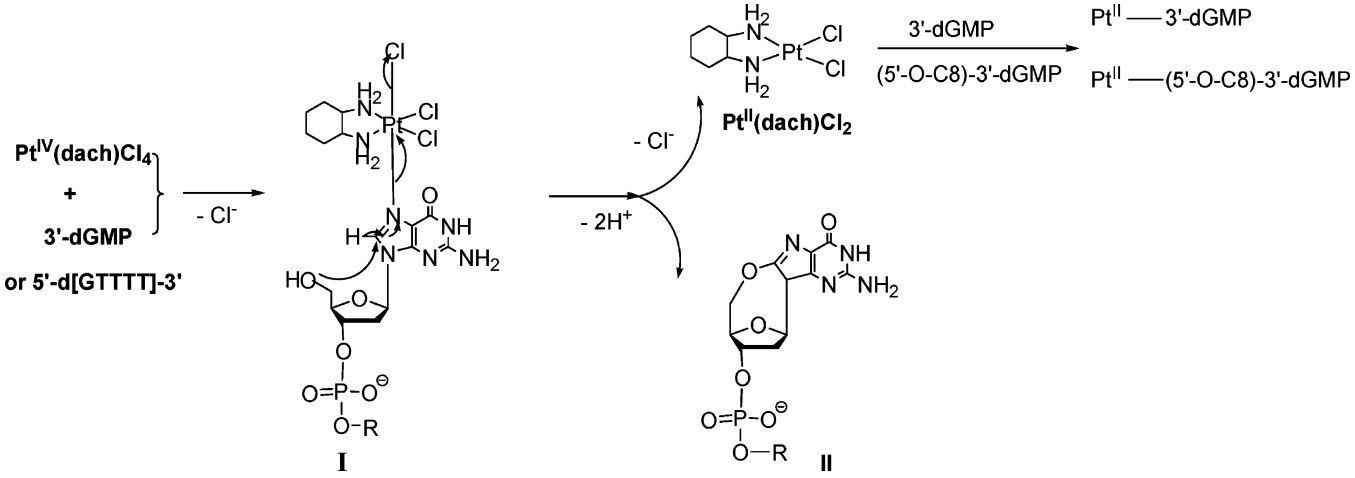

of 8-oxo-G was observed in all the oligonucleotides studied. However, 8-oxo-G was not detected when the reaction was gel-filtered prior to enzyme digestion. Therefore, we conclude that 8-oxo-G was generated from the reaction between the monomeric 5′-dGMP generated by enzyme digestion of oligomers and the excess $[Pt^{IV}Cl_4(dach)]$ during the enzyme digestion.

Although others have reported that some Pt^{IV} complexes directly bind to N7 of guanine derivatives to form a $Pt^{IV}-G$ adduct,[8] no oxidation of nucleobases by Pt^{IV} complexes has been reported except 5′-dGMP[5] and 3′-dGMP reactions with $[Pt^{IV}Cl_4(dach)]$. We hypothesize that, for the stoichiometric redox reaction to occur, the internal electron-transfer step between the G ligand and the Pt^{IV} ion must be fast. For the fast internal electron transfer, two requirements have to be satisfied. First, the C8 of deoxyguanosine or guanosine has to be highly positively polarized. Because $[Pt^{IV}Cl_4(dach)]$ has a high reduc-

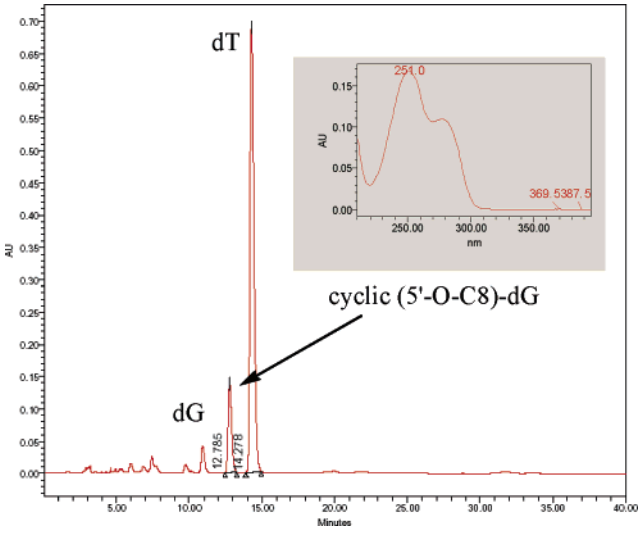

Figure 13. HPLC chromatogram (DAD, $\lambda = 260$ nm) of the digested 2 day reaction of 10 mM [$Pt^{IV}Cl_4$(dach)] with 1.0 mM 5′-d[GTTTT]-3′ at pH 7.4 ($t = 0$) and 37 °C.

Scheme 2. Internal Electron Transfer through Cyclization

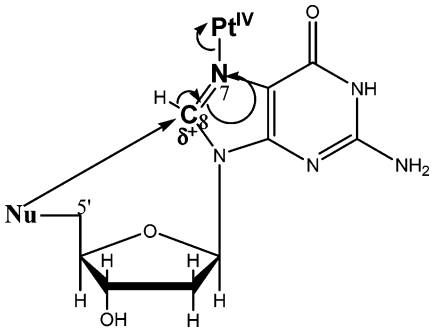

tion potential ($E_{1/2} = -90$ mV)[13] when it binds to N7-G, it withdraws electron density from the C8-G far more than other Pt^{IV} complexes with lower reduction potentials. Second, G has to have a good nucleophile such as phosphate or hydroxyl at the 5′-position, which attacks C8-G to form a cyclic intermediate and transfer the electron to Pt^{IV} ion (Scheme 2).

The [$Pt^{IV}Cl_4$(dach)]/5′-dGMP (3′-dGMP or 5′-d[GTTTT]-3′) system satisfies both requirements, and the redox reaction occurred efficiently. Many other reactions between Pt^{IV} complexes and G derivatives reported in the literature did not show this redox reaction because the reactions did not meet the two requirements. For example, Pt^{IV} complexes which have low reduction potentials such as *cis*,*cis*,*trans*-[$Pt^{IV}Cl_2(OCOCH_3)_2(NH_3)$(c-$C_6H_{11}NH_2$)][8b] and [$Pt^{IV}(OCOCH_3)_4$(en)][8e] only bind to N7 of 5′-dGMP. When [$Pt^{IV}Cl_4$(en)], which has a moderate reduction potential ($E_{1/2} = -160$ mV)[13] reacted with 5′-GMP, it produced less than 20% of the oxidized 5′-GMP compared to [$Pt^{IV}Cl_4$(dach)].[5c] Several Pt^{IV} complexes with a relatively high reduction potential such as *cis*-[$Pt^{IV}Cl_2(NH_3)_4$] and *cis*-[$Pt^{IV}(NH_3)$(cha)Cl_4] only bind to N7 of 9-Mxan.[8d]

The identity of the final oxidized G depends on the hydrolysis rate of the cyclic intermediate. The cyclic phosphodiester intermediate formed from [$Pt^{IV}Cl_4$(dach)]/5′-dGMP is hydrolyzed to 8-oxo-5′-dGMP. However, the cyclic ether intermediate formed from [$Pt^{IV}Cl_4$(dach)]/3′-dGMP or 5′-d[GTTTT] does not hydrolyze, and the cyclic form is the final oxidation product.

In summary, we have demonstrated that [$Pt^{IV}Cl_4$(dach)] oxidizes G in 3′-dGMP and 5′-d[GTTTT]-3′ by nucleophilic attack of the 5′-OH to C8 to form a cyclic (5′-O-C8)-ether. The mechanism allows us to predict if a Pt^{IV} complex can oxidize a certain guanosine derivative. For the redox reaction to occur, the Pt^{IV} complex has to have a high reduction potential, and the G derivative has to have a nucleophile such as a phosphate or hydroxyl group.

Experimental Section

Materials. [$Pt^{IV}Cl_4$(dach)] (tetraplatin) was obtained from the National Cancer Institute, Drug Synthesis and Chemistry Branch, Developmental Therapeutics Program, Division of Cancer Treatment. 5′-dGMP, 3′-dGMP, cGMP, and 9-Mxan were purchased from Sigma-Aldrich. Oligonucleotides were purchased from IDT Technologies. Alkaline phosphatase and P1 nuclease were obtained from Roche and ICN Biochemicals, respectively.

Reaction Preparation. Buffers were not used in order to avoid complications arising from buffer coordination to platinum.[14] Stock solutions (11 mM) of [$Pt^{IV}Cl_4$(dach)] were prepared by dissolving 11 μmol of the Pt^{IV} compound in 1 mL of H_2O in an amber vial. The dissolution of [$Pt^{IV}Cl_4$(dach)] is slow, so several heating (maximum 50 °C) and vortexing cycles over 5 or 6 h were necessary for complete dissolution. After the Pt^{IV} compound was dissolved, an appropriate amount of guanine stock solution was added to give the desired final concentration. The pH of the solution was adjusted to pH 8.6 with 0.1 M NaOH. The time when the pH was adjusted to pH 8.6 was recorded as the beginning of the reaction. All the samples for NMR analysis were prepared in D_2O (>98%). Reaction solutions were filtered through a syringe-end filter disk (Gelman Acrodisk 0.45 μm pore size) before HPLC and NMR analysis.

Enzyme Digestion of Oligonucleotides. Unreacted [$Pt^{IV}Cl_4$(dach)] was removed using a Sephadex GM-25 resin. The samples were treated with Nuclease P1 (20 units/nmol of DNA) at pH 5.3 using 0.1 M ammonium acetate buffer, and were incubated at 45 °C for 6 h. The pH of the solution was readjusted to 7.87 with 0.1 M Tris buffer (pH 8.5), alkaline phosphatase (1 unit/nmol of DNA) was added, the resulting solution was incubated at 37 °C for 12 h. The phosphatase removes inorganic phosphate from the newly cleaved nucleotides. Dephosphorylating buffer was added in the same quantity as the alkaline phosphatase, and the resulting solution was incubated for 6 h at 37 °C.

pH and Chloride Concentration. The pH and chloride concentration were measured with pH and chloride (Orion Model 94-17B) electrodes, respectively, connected to a pH meter (Orion Research 960).

HPLC. HPLC measurements were performed on a Waters Alliance 2695 apparatus equipped with a Waters 2996 DAD and a Waters Atlantis dC18 (5 μm, 4.6 mm × 250 mm) column. Typical solvent conditions included 97% ammonium acetate (20 mM, pH 4.2) and 3% acetonitrile at 1 mL/min with a column temperature of 35 °C.

NMR. NMR spectra were recorded on a Bruker NMR spectrometer equipped with a broad-band inverse tunable probe operating at 400.13 MHz for ^{1}H and 161.97 MHz for ^{31}P. Chemical shifts for ^{1}H and ^{31}P are reported relative to the peaks for tetramethylsilane (TMS) and 85% H_3PO_4, respectively, each at 0.00 ppm. Samples were prepared in D_2O, and the residual water signal was further suppressed by the Watergate pulse sequence.[15] Time-course experiments were performed at 37 °C by recording spectra at 1 h intervals by use of a multiple acquisition

(13) Choi, S.; Filotto, C.; Bisanzo, M.; Delaney, S.; Lagasee, D.; Whitworth, J. L.; Jusko, A.; Li, C.; Wood, N. A.; Willingham, J.; Schwenker, A.; Spaulding, K. *Inorg. Chem.* **1998**, *37*, 2500−2504.

(14) (a) Lempers, E. L. M.; Bloemink, M. J.; Reedijk, J. *Inorg. Chem.* **1991**, *30*, 201−206. (b) Barnham. K. J.; Guo, Z.; Sadler, P. J. *J. Chem. Soc., Dalton Trans.* **1996**, 2867−2876.

(15) Trimble, L. A.; Bernstein, M. A. *J. Magn. Reson., Ser. B* **1994**, *105*, 67−72.

program (total acquisition time + delay between experiments = 1 h) with 256 scans for ^{1}H or 1000 scans for ^{31}P with broad-band ^{1}H decoupling.

MS. *m*/*z* was obtained using MALDI-TOF-MS at the Molecular Biology Core Facility, Dartmouth Medical School. Spectra were recorded in negative ion mode with an accelerating voltage of 20000 V, a grid voltage at 65%, a guide wire at 0.05%, and an extraction delay time of 50 ns. The acquisition range was 325−365 amu with 200 laser shots/spectrum at a repetition rate of 20.0 Hz. The matrix used to aid in the acquisition was 3-hydroxypicolinic acid.

Acknowledgment. This work was supported by donors of the Petroleum Research Fund, administered by the American Chemical Society (Grant PRF-37873-B3), and the Vermont Genetics Network through the NIH (Grant 1 P20 RR16462 from the BRIN program of the National Center for Research Resources). Special thanks goes to Dr. Steve Bobbin at the Molecular Biology Core Facility, Dartmouth Medical School, for the MALDI-TOF MS spectra.

JA045194N